(Hyper)nuclei and anti-(hyper)nuclei production in Pb–Pb collisions in ALICE at LHC

Manuel Colocci (for the ALICE Collaboration)

Dipartimento di Fisica dell'Università di Bologna and INFN-sezione di Bologna. Via Irnerio 46, 40126 Bologna, Italy

E-mail: manuel.colocci@cern.ch

Abstract. The ALICE detector at the LHC is used to study Pb–Pb collisions at $\sqrt{s_{\rm NN}} = 2.76$ TeV. At this energy almost equal amounts of matter and anti-matter are produced in the central rapidity region. This in turn enables the production of (hyper)nuclei and anti-(hyper)nuclei, which are measured with nearly identical abundances. Thanks to its high quality tracking and particle identification capabilities, the ALICE detector allows the investigation of these rarely produced (anti-)matter states. Preliminary results on the production of light (anti-)nuclei and (anti-)hypernuclei, and a search for exotic bound states are discussed in this article.

1. Introduction

In relativistic heavy-ion collisions a large amount of (kinetic) energy may be deposited in a small volume, allowing for creation of the Quark-Gluon Plasma[1] (QGP), a phase of matter in which the quark and gluon degrees of freedom normally confined within hadrons are mostly liberated. The created system expands and cools down after its production, and the transition into an hadron gas occurs. In the final state of this process a large amount of light (anti-)nuclei and (anti-)hypernuclei is also formed[2, 3]. Thanks to its precise tracking and particle identification capabilities, the ALICE experiment[4] successfully records these produced (anti-)matter states giving the opportunity to investigate their production mechanisms: actually, an (hyper)nucleus is supposedly formed by a coalescence process of two or more (anti-)baryons at the last stage of the collision[5] and/or during the hadronization process at the chemical freeze-out of the QGP[6]. Furthermore, the large amount and similar abundance of matter and anti-matter nuclei observed by the ALICE experiment, allows the investigation of other key features of light nuclei as mass and lifetime. The measurement of the production and properties of light nuclei could also provide useful information for the search of the anti-matter in the universe and, in particular, for the potential detection of the dark matter with hypothetical decays into anti-deuteron[7].

2. (Anti-)nuclei

The identification of (anti-)nuclei is possible via their specific energy loss measurement ($\mathrm{d}E/\mathrm{d}x$) provided by the Time Projection Chamber[8] (TPC) of the ALICE experiment. ^{3}He nucleus is identified in a wide range of the transverse momenta, up to $p_{\rm T} \simeq 8$ GeV/c, the deuteron up to $p_{\rm T} \simeq 1.5$ GeV/c, requiring that the energy deposit of each track is compatible, within 3σ (where σ is the standard deviation), with the expected value for a given species. To extend the deuteron

identification up to about $p_{\mathrm{T}} \simeq 4.5$ GeV/c, the measurement of its velocity provided by the Time Of Flight[9] (TOF) detector is used as well. The ALICE experiment is also equipped with the High Momentum Particle Identification (HMPID) system which is a ring-imaging Cherenkov detector covering a limited acceptance region. Employing it, it is possible to further enlarge the transverse momentum region where the deuteron is identified, up to $p_{\mathrm{T}} \simeq 8$ GeV/c in the most central events (in the $0-10\%$ centrality class), where significant statistics are collected. A large amount of the nuclei detected in this way at low p_{T} (up to about 1.5 GeV/c for deuteron and about 2 GeV/c for ^{3}He) is created in secondary collisions (material "knock out") and not in the primary interactions. In order to separate this component, the measurement of the Distance of Closest Approach (DCA) to the primary vertex provided by the Inner Tracking System[10] (ITS) is used. A cut of 1 cm on the projection of the DCA along the beam-pipe direction is applied and its second component lying in the transverse plane is fitted with two different Monte-Carlo templates to remove the remaining contamination. Fig. 1 and Fig. 2 show the preliminary spectra of deuteron and ^{3}He nucleus as a function of p_{T} and the centrality class of events, already corrected for tracking efficiency and acceptance. The corresponding anti-particle spectra are not shown due to large uncertainties on the description of their interaction with the detector material. The spectra are fitted with a blast-wave function[11], that assumes a thermal emission of particles from an expanding source. The mean $\langle p_{\mathrm{T}} \rangle$ of deuterons and ^{3}He increases with centrality as already observed for lighter particles such as pions, kaons and protons. This trend can generally be explained as a consequence of the expanding source[12].

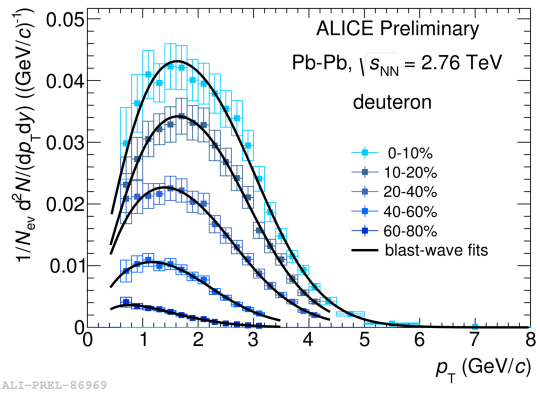

Figure 1. Deuteron spectra. The statistical and systematic uncertainties are reported with a vertical line and an open box, respectively.

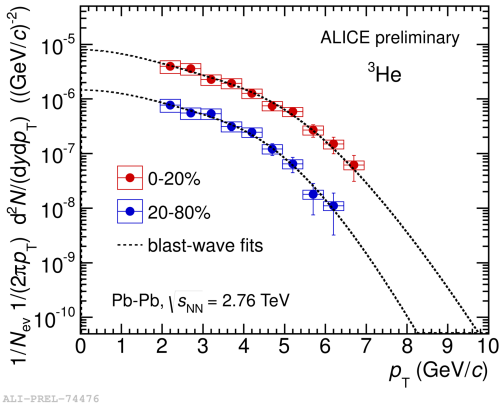

Figure 2. ^{3}He spectra. As done for the deuteron, also the fit with an hydrodynamical model (blast-wave) is performed.

An analysis of the 2011 Pb–Pb data, which is the bulk of the statistics, also reveals 10 candidate $^4\overline{\mathrm{He}}$ nuclei. The identification strategy is based on an offline trigger which accepts only tracks with a TPC dE/dx corresponding to a $^3\overline{\mathrm{He}}$ (within 3σ) or to a heavier anti-nucleus, and on the measurement of the mass-over-charge of the anti-particles, obtained using the TOF detector. The $p_{\mathrm{T}}-$integrated yields of p, d, ^{3}He and $^4\overline{\mathrm{He}}$ as a function of their mass are reported in Fig. 3. A decreasing exponential behavior is observed and a preliminary reduction factor for each additional (anti-)nucleon of about 300 is obtained. This implies that the generation of the next stable anti-matter nucleus ($^6\overline{\mathrm{Li}}$) is not reachable with the current available statistics.

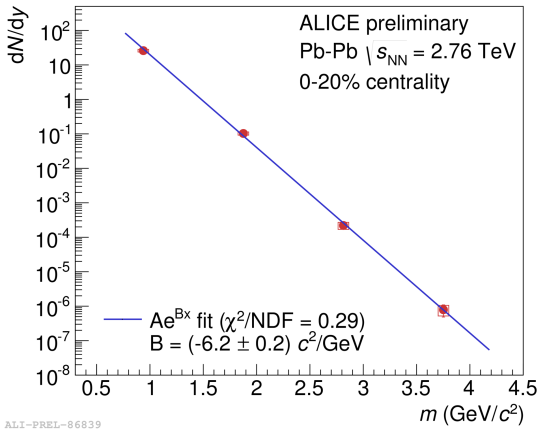

Figure 3. $p_{\mathrm{T}}-$integrated yields of p, d, ^{3}He and $^4\overline{\mathrm{He}}$ in the $0-10\%$ centrality class. The blue line is the fit with the function $\mathrm{A}e^{\mathrm{B}m}$.

3. (Anti-)hypermatter

In high energy Pb–Pb collisions strange quarks are produced abundantly compared to elementary pp collisions. Consequently, an enhanced production of hypernuclei is expected. The lightest known hypermatter nucleus is the hypertriton ($^3_\Lambda$H), formed by a proton, a neutron and a Λ particle. This nucleus and the corresponding anti-particle, the anti-hypertriton ($\overline{^3_\Lambda\mathrm{H}}$), are reconstructed via their decay channel $^3_\Lambda\mathrm{H} \rightarrow {}^3\mathrm{He} + \pi^-$ ($\overline{^3_\Lambda\mathrm{H}} \rightarrow \overline{^3\mathrm{He}} + \pi^+$). Both daughter particles are identified via the TPC $\mathrm{d}E/\mathrm{d}x$ measurement and with a series of topological cuts: a maximum DCA between the ^{3}He and π candidates ($< 0.7\sigma$), a minimum DCA of pions from the primary vertex (> 0.4 cm), and a maximum pointing angle between the line joining the primary and secondary vertex and the total momentum (< 0.05 rad). In Fig. 4 the invariant mass distribution of $(^3\mathrm{He}+\pi^-)+(\overline{^3\mathrm{He}}+\pi^+)$ is shown. The signal (filled black points) is extracted from the data by subtracting the corresponding background (red histogram). This background is estimated from the like-sign distribution $(^3\mathrm{He}+\pi^+)+(\overline{^3\mathrm{He}}+\pi^-)$. With this technique the $^3_\Lambda$H and $\overline{^3_\Lambda\mathrm{H}}$ are clearly identified in central and semi-central collisions in a wide momentum range ($2 < p_{\mathrm{T}} < 10$ GeV/c). The comparison of the hypertriton yield with predictions from statistical thermal models[13, 14] with various assumptions of freeze-out conditions is shown in Fig. 5. The preliminary comparison favours a model that requires thermal equilibrium during the hadronization process with a chemical freeze-out temperature $T_{ch} = 156$ MeV. The lifetime of hypertriton is preliminary measured: $\tau = 181 \pm 44(\mathrm{stat.}) \pm 29(\mathrm{syst.})$ ps, compatible with the existing experimental results. This is obtained via the decay law $N(t) = N(0)e^{-t/\tau}$ where $t = l/(\beta\gamma c)$ and $\beta\gamma c = p/m$, l being the decay length, p the momentum and m the $^3_\Lambda$H mass.

The investigation of (anti-)hypermatter is also extended to two exotic hypothetical states: the $\overline{\Lambda\mathrm{n}}$ and the H-dibaryon. The first is searched for the expected decay $\overline{\Lambda\mathrm{n}} \rightarrow \mathrm{d} + \pi^-$ with a similar experimental technique employed as for the hypertriton measurement. The investigation is made only for the $\overline{\Lambda\mathrm{n}}$ state excluding its matter counterpart (Λn) because of the lower background corresponding to the particle "knock-out" from the detector material. The second, the H-dibaryon, is a hypothetical state of uuddss ($\Lambda\Lambda$) first predicted in [15] via bag model calculations. Its search is made in the channel $\mathrm{H}(\Lambda\Lambda) \rightarrow \Lambda + \mathrm{p} + \pi$. The analysis strategy is analogous to the $\overline{\Lambda\mathrm{n}}$ state, with the exception that a second V^0 decay has to be identified. No significant signal is observed in the invariant mass distributions of these exotic states. It is therefore only possible to set upper limits on the production yields of these hypothetical states. They are more than a factor 10 below the statistical thermal model predictions which, on the other hand, are in agreement with the measurement of the production yield of d, ^{3}He and (anti-)$^3_\Lambda$H[16].

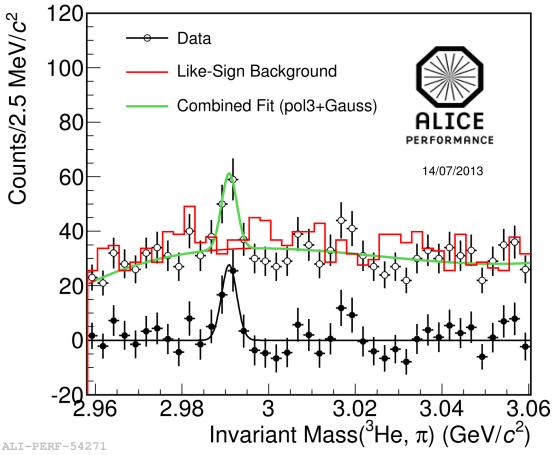

Figure 4. Invariant mass distribution of $(^3\mathrm{He} + \pi^-) + (^3\overline{\mathrm{He}} + \pi^+)$. See text for more details.

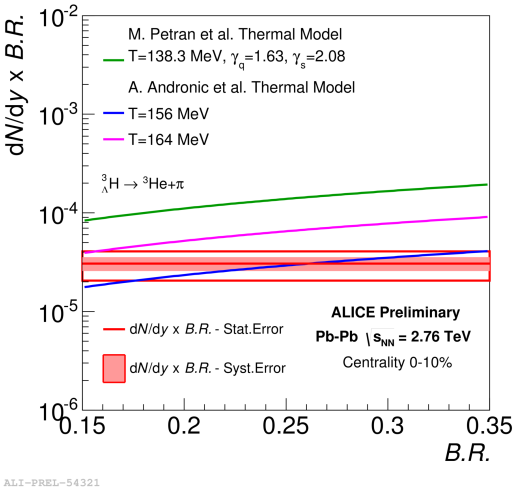

Figure 5. Production yield dN/dy of $^3_\Lambda$H (not corrected for the B.R.) compared to expectations from statistical thermal models.

4. Summary and perspectives

Preliminary ALICE results for light (hyper)nuclei in Pb–Pb collisions at $\sqrt{s_{\mathrm{NN}}} = 2.76$ TeV have been presented. During the forthcoming LHC Run-II data taking the precision of the current measurements could significantly improve due to the expected increase of event statistics. The measurement of the (anti-)hypertriton will be performed in other decay channels and multi-strange anti-hypernuclei could be observed. The search for (anti-)hypermatter will be extended to other hypothetical exotic states.

[1] Braun-Munzinger P, Stachel J 2007 *Nature* **448** 302.
[2] Agakishiev H *et al.* (STAR Collaboration) 2011 *Nature* **473** 353.
[3] Abelev B I *et al.* (STAR Collaboration) 2010 *Science* **328** 58.
[4] Abelev B I *et al.* (ALICE Collaboration) 2014 *Int. J. Mod. Phys. A* **29** 1430044.
[5] Xue L, Ma Y G, Chen J H, Zhang S 2012 *Phys. Rev. C* **85** 064912.
[6] Andronic A, Braun-Munzinger P, Stachel J, Stocker H 2011 *Phys. Lett. B* **697** 203.
[7] Donato F, Fornengo N, Salati P 2000 *Phys. Rev. D* **62** 043003.
[8] Alme J *et al.* 2010 *Nucl. Instrum. Meth. A* **622** 316.
[9] Akindinov A *et al.* 2013 *Eur. Phys. J. Plus* **128** 44.
[10] Contin G 2012 *JINST* **7** C06007.
[11] Schnedermann E, Sollfrank J, Heinz U W 1993 *Phys. Rev. C* **48** 2462.
[12] Abelev B I *et al.* (ALICE Collaboration) 2012 *Phys. Rev. Lett* **109** 252301.
[13] Petran M, Latessier J, Petracek V, Rafelski J 2013 *Phys. Rev. C* **88** 034907.
[14] Andronic A, Braun-Munzinger P, Stachel J 2009 *Phys. Lett. B* **673** 142.
[15] Jaffe R L 1977 *Phys. Rev. Lett.* **38** 195, 1977 *erratum ibid.* **38** 617.
[16] Floris M 2014 *Nucl. Phys. A* **931** 103.